Correlation between Mn oxidation state and magnetic behavior in Mn/ZnO multilayers prepared by sputtering

Cite as: J. Appl. Phys. **102**, 033907 (2007); https://doi.org/10.1063/1.2764207
Submitted: 02 April 2007 . Accepted: 14 June 2007 . Published Online: 03 August 2007

E. Céspedes, J. Garcia-Lopez, M. García-Hernández, A. de Andrés, and C. Prieto

Correlation between Mn oxidation state and magnetic behavior in Mn/ZnO multilayers prepared by sputtering

E. Céspedes
Instituto de Ciencia de Materiales de Madrid, Consejo Superior de Investigaciones Científicas, Cantoblanco, Madrid, 28049, Spain

J. Garcia-Lopez
Centro Nacional de Aceleradores, Avenida Thomas A. Edison, Isla de la Cartuja, Sevilla, 41092, Spain

M. García-Hernández, A. de Andrés, and C. Prieto
Instituto de Ciencia de Materiales de Madrid, Consejo Superior de Investigaciones Científicas, Cantoblanco, Madrid, 28049, Spain

(Received 2 April 2007; accepted 14 June 2007; published online 3 August 2007)

Compositional, microstructural, and magnetic characterization of $[\mathrm{ZnO}(30\ \text{Å})/\mathrm{Mn}(x)]_n$ multilayers prepared by sputtering is presented to study the observed ferromagnetism in the Mn-ZnO system. The nominal Mn layer thickness, x, is varied from 3 to 60 Å, while the number of bilayers, n, is increased to maintain the total amount of Mn constant. Microstructure information was deduced from x-ray reflectivity, Mn oxidation state was determined by x-ray absorption spectroscopy, and magnetic properties were measured over a temperature range of 5–400 K. Magnetic behavior of these samples is found to be related to the Mn layer thickness (x). Multilayers with $x \geq 30$ Å exhibit ferromagnetism with a Curie temperature above 400 K, while mostly paramagnetic behavior is obtained for $x < 15$ Å. Magnetic behavior is discussed in terms of electronic and structural parameters of samples. Mn-ZnO interface effect is related to the ferromagnetic order of the samples, but it is not a sufficient condition. The essential role of the Mn oxidation state in the magnetic behavior of this system is pointed out. It is shown a correlation between the obtained ferromagnetism and a Mn oxidation state close to 2+. © *2007 American Institute of Physics*. [DOI: 10.1063/1.2764207]

I. INTRODUCTION

Recently, Mn-Zn-O system has attracted much attention because of the theoretical predictions of room temperature ferromagnetism in Mn-doped ZnO as a wide band gap diluted magnetic semiconductor (DMS).[1] In the last years, there has been reported either paramagnetism[2] or ferromagnetism in the $Zn_{1-x}Mn_xO$ family, with Curie temperatures over room temperature for films grown by different deposition techniques.[3,4] However, experimental results are very different and even contradictory and the origin of the reported ferromagnetic properties still remains a matter of discussion. In many cases, insufficient structural studies give rise to these discrepant results, showing that a variety of characterizations of these complex materials is fundamental to find defensible structure-function relationships.[5]

The preparation of manganese zinc oxide films allows studying Mn-ZnO interface, that is one of the most intriguing problems in the field that both theoreticians and experimentalists are dealing with.[6,7] Multilayer structures preparation has been reported for Co/ZnO thin films[8,9] and also for Co-Fe/ZnO thin films grown by ion beam assisted sputtering,[10] obtaining ferromagnetic phases. However, there has not been reported any study in the Mn/ZnO multilayer system.

In this article, we present the magnetic characterization and its correlation with the Mn oxidation state of a multilayer series having constant width of ZnO layers and variable thickness of Mn layers. The number of bilayers has been progressively modified to have constant Mn amount in the film. Therefore, the Mn-ZnO interface effect is studied to clarify its relevant role in the magnetic properties of this system.

II. EXPERIMENT

Multilayer films were prepared using dc sputtering by sequential deposition of ZnO and Mn on Si(100) substrates at room temperature. The sputtering system allows controlling the movement of the sample-holder disk and the time (as well as the sputtering working gas) it is placed on each sputtering (or presputtering) position automatically. The residual pressure was near 1×10^{-7} mbar. ZnO layers were deposited by reactive sputtering from a pure Zn target (99.9%) using a O_2/Ar mixture gas (43% O_2-rich) at a working pressure of 5.4×10^{-3} mbar. Mn layers were grown from a Mn target (99.95%) at 5.0×10^{-3} mbar pressure of pure Ar. Presputtering was developed not only before the multilayer growth but also between two consecutive layers. Deposition rates were about 0.07 nm/s for Mn and 0.05 nm/s for ZnO. After calibration procedures, the nominal bilayer thickness of the studied samples are summarized in Table I; for all of them, multilayer structure fabrication began with ZnO layer and a last additional layer (30 Å thick) was deposited on top.

Low angle x-ray reflectivity (XRR) measurements were carried out on a Bruker D8 X-ray diffractometer with a

TABLE I. Multilayer series summary. Bilayer thickness has been determined from simulation of XRR spectra, Mn atomic density, and sample composition have been obtained from simulation of Rutherford backscattering spectroscopy (RBS) data and Mn oxidation states have been estimated from the *K*-edge energy shifts from XANES spectra.

Sample (nominal thickness)	Bilayer thickness (Å)	Mn-layer atomic density (10^{15} at./cm^2)	Composition (%)			Mn oxidation state
			[Mn]	[Zn]	[O]	
(30 Å ZnO/60 Å Mn)$_5$	128	185.5	0.35	0.12	0.53	+2.1±0.2
(30 Å ZnO/30 Å Mn)$_{10}$	87	262.0	0.35	0.16	0.49	
(30 Å ZnO/15 Å Mn)$_{20}$	63	262.0	0.25	0.22	0.53	+2.6±0.2
(30 Å ZnO/7 Å Mn)$_{43}$	47	326.8	0.19	0.29	0.52	+2.9±0.2
(30 Å ZnO/4 Å Mn)$_{75}$	40	405.0	0.16	0.33	0.51	
(30 Å ZnO/2 Å Mn)$_{75}$	37	315.0	0.13	0.34	0.53	
(30 Å ZnO/1 Å Mn)$_{75}$	34	255.0	0.11	0.34	0.55	+3.3±0.2

Cu $K\alpha$ source. Rutherford backscattering spectroscopy (RBS) experiments were made at the Centro Nacional de Aceleradores at Sevilla. The magnetic characterization was performed by means of a SQUID magnetometer (MPMS-5S from Quantum Design). Finally, x-ray absorption spectroscopy (XAS) experiments were carried out in fluorescence detection mode at the European Synchrotron Radiation Facility (BM26A) at Grenoble.

III. RESULTS AND DISCUSSION

Figure 1 shows the XRR characterization of samples. Independently of the bilayer thickness, all of them exhibit multilayer periodicity. This heterostructure feature indicates that, actually, samples are formed by separated Mn and ZnO-rich regions; this fact makes possible the study of the magnetic behavior of samples with the same Mn amount but different Mn-ZnO interfaces. The simulation of the reflectivity data, performed by the Xrealm software provides microstructural information as bilayer thickness and roughness. Bilayer thickness results, summarized in Table I, are mostly in agreement with nominal values. Additionally, the obtained roughness is about 7 Å for every sample indicating that in multilayers with layer thickness below this value Mn layers become noncontinuous allowing clustering formation.

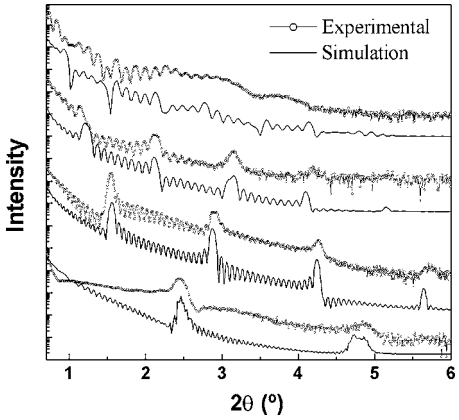

FIG. 1. X-ray reflectivity multilayer spectra and simulations. From top to bottom spectra of samples (30 Å ZnO/60 Å Mn)$_5$, (30 Å ZnO/15 Å Mn)$_{20}$, (30 Å ZnO/7 Å Mn)$_{43}$, and (30 Å ZnO/2 Å Mn)$_{75}$. All spectra have been vertically shifted for clearness.

RBS experiments were performed to evaluate the actual amount of Mn in each sample as well as film atomic composition. Figure 2 shows experimental data and simulations of some samples, Fig. 2(a) points up simulations of data obtained with incident ions of 2 MeV in order to obtain film composition.

Additionally, RBS spectra have been collected with incident ions of 8 MeV to distinguish the Mn and Zn contributions, as it can be observed in Fig. 2(b). For these energies, Mn and Zn cross sections are not known and simulation

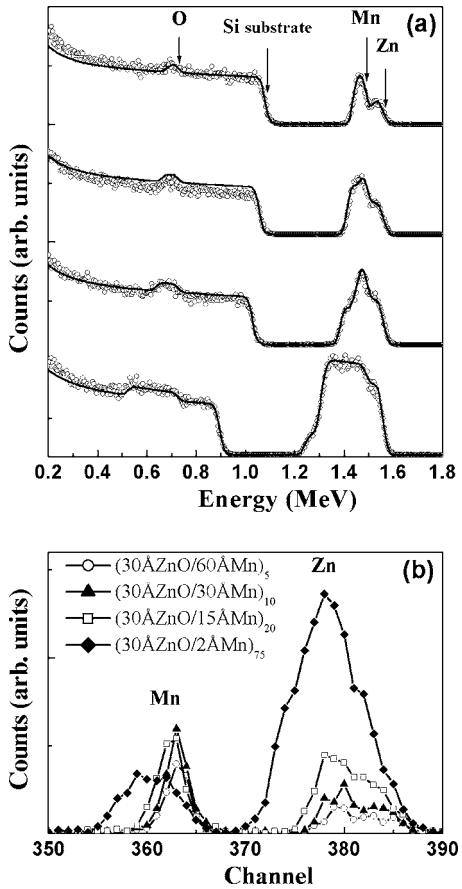

FIG. 2. (a) RBS spectra taken at energy of incident ions of 2 MeV (dots) and their simulations (lines) of samples (30 Å ZnO/60 Å Mn)$_5$, (30 Å ZnO/15 Å Mn)$_{20}$, (30 Å ZnO/7 Å Mn)$_{43}$, and (30 Å ZnO/1 Å Mn)$_{75}$, from top to bottom. All spectra have been vertically shifted for clearness. (b) RBS spectra of the same samples at 8 MeV.

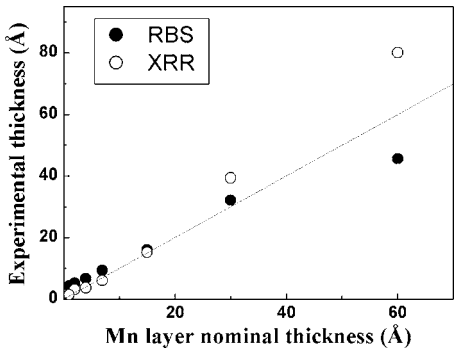

FIG. 3. Comparison between experimental Mn layer thickness values obtained from RBS and XRR (straight line represents correspondence between both values).

cannot be performed in a similar way to the spectra collected at 2 MeV. However, the Mn/Zn ratio can be calculated because it is proportional to the integral ratio of both contributions, which become well separated at 8 MeV. Therefore, we can use the Mn/Zn ratio in sample (30 Å ZnO/60 Å $Mn)_5$ obtained with 2 MeV (where both concentrations can be obtained by simulation) to calculate the actual ratio in the whole set of samples. After analysis of the two used energies, the obtained film composition is given in Table I.

The comparison between the Mn layer thicknesses obtained by XRR simulations and the calculated ones by taking into account the RBS results (where the metallic Mn density has been used) is shown in Fig. 3. The most noticeable detail is that, for thick enough nominal Mn layer samples, XRR determined Mn-layer thickness is higher than the corresponding value obtained from RBS. As XRR is a direct measurement of thickness, this discrepancy should be explained because, in the thickness calculation from RBS data, the used metallic Mn density is, in fact, higher than the actual one, pointing toward an oxidized Mn layer. The relationship between the straight-line slopes corresponding to both techniques may be used to fit the average Mn layer density in the samples. The obtained slope of 4.4×10^{22} at./cm^3 is clearly smaller than the value corresponding to metallic Mn (8.1×10^{22} at./cm^3). A comparison with some manganese oxides such as MnO (4.6×10^{22} at./cm^3), Mn_2O_3(1.9×10^{22} at./cm^3), or MnO_2(3.5×10^{22} at./cm^3) indicates that Mn is present as a partially oxidized form.

Figure 4(a) shows the magnetization variation with temperature $M(T)$ from 5 to 400 K of some selected samples. Room temperature ferromagnetism is clearly observed for the thickest Mn-layer film. As the Mn layer thickness decreases, a reduction of magnetization takes place, exhibiting paramagneticlike behavior for samples with the thinnest Mn layers. Magnetization per manganese atom has been calculated taking into account the precise amount of Mn obtained by RBS. The possibility of ferromagnetism due to any magnetic impurity in the samples can be ruled out here: First, x-ray absorption experiments performed at L edges have revealed that no appreciable Fe, Co, or Ni contamination is present in the films.[11] Besides, the behavior of $M(T)$ supports the fact that ferromagnetism does not come from uncontrolled magnetic impurities from the starting Mn target. $M(T)$ normalized to the total number of Mn atoms (and consequently to the expected number of impurity atoms) exhibits magnetization magnitudes that are different for the studied set of samples and follow a monotonous layer thickness dependence. This fact allows us to discard ferromagnetism from uncontrolled impurities, the case where magnetization would be proportional to the impurity amount.

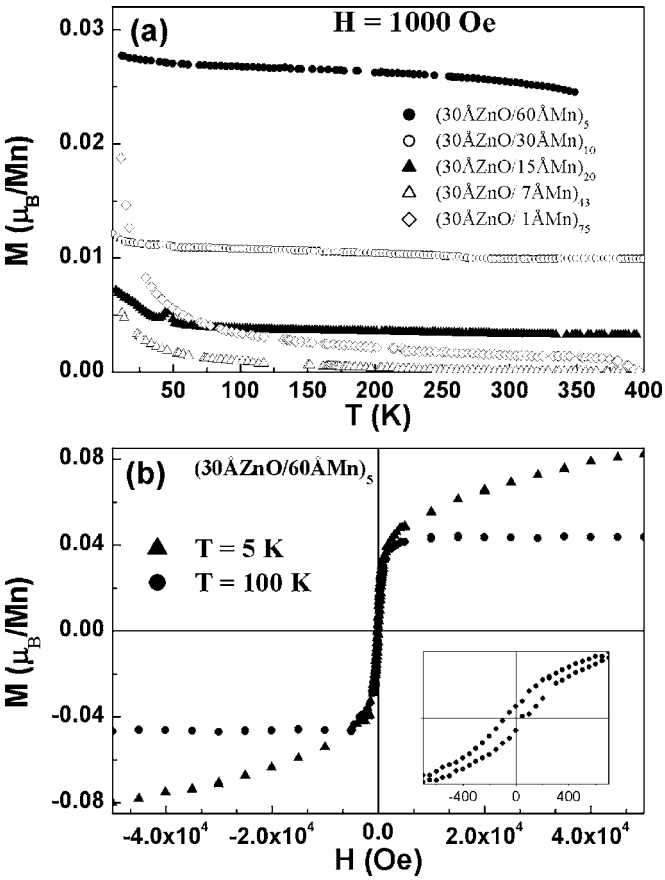

FIG. 4. (a) Magnetization curves vs temperature. (b) Hysteresis loops at 5 and 100 K of sample (30 Å ZnO/60 Å $Mn)_5$. The inset shows the 100 K hysteresis loop.

To study film ferromagnetism, hysteresis loops have been measured at several temperatures. Figure 4(b) shows the magnetic hysteresis loops obtained at 5 and 100 K for film (30 Å ZnO/60 Å $Mn)_5$. The substrate diamagnetic background has been subtracted at the plot. This sample presents nearly 0.05 μ_B per Mn atom, being the highest saturation magnetization in this series. The obtained coercive field at 100 K is about 80 Oe [inset of Fig. 4(b)].

In order to compare directly these magnetic values with other reported ones for the Mn/ZnO system, due to differences in reporting M_S in the literature, it is necessary to take into account different normalizations. Then, for comparison purposes, we have also normalized the obtained M_S at 100 K ($M_S\sim0.05$ μ_B/Mn) by considering the film volume ($M_S\sim10$ emu/cm^3) and the total Mn mass ($M_S\sim4$ emu/g of Mn).

This value, as well as the hysteresis loop shape, is comparable to those previously reported: in Ref. 6, a saturation magnetization of 1 emu/cm^3 and a coercive force around 50 Oe at 5 K are found for a thin film multilayer ZnO/MnO_2; in Ref. 16, M_S of 0.28 emu/g and H_C of 78 Oe at 10 K have

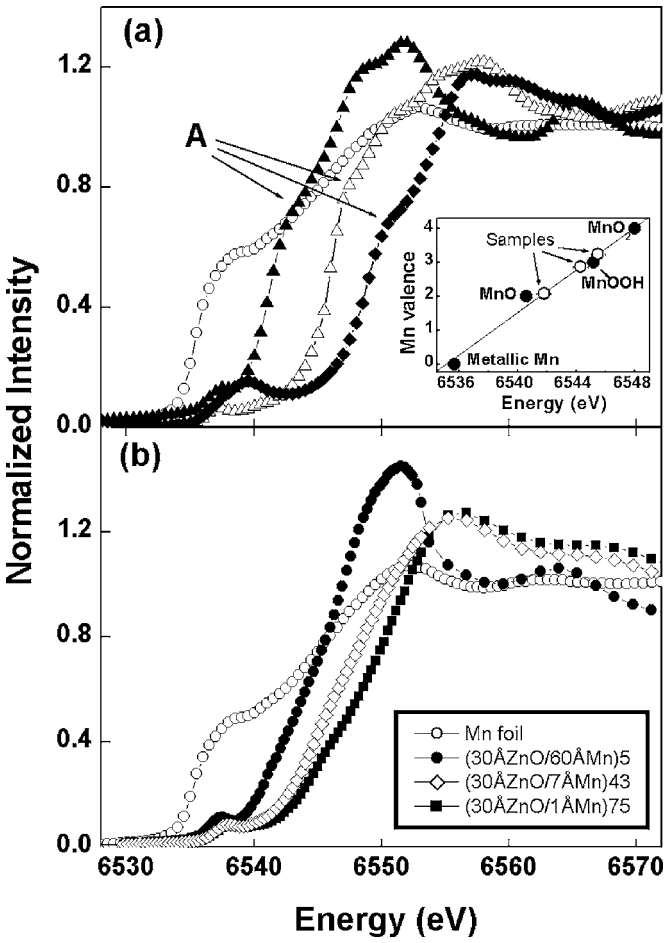

FIG. 5. (a) Mn *K*-edge spectra of Mn foil, MnO, MnOOH, and MnO_2, from left to right (taken from Ref. 12). Inset: Mn-valence vs the threshold energy (● references and ○ samples). (b) Experimental Mn *K*-edge spectra of Mn foil, and (30 Å ZnO/60 Å Mn)$_5$, (30 Å ZnO/7 Å Mn)$_{43}$, and (30 Å ZnO/1 Å Mn)$_{75}$ samples (from left to right). Pre-edge background subtraction and edge step normalization procedures were performed on each spectrum.

been obtained for nanosized $Zn_{0.95}Mn_{0.05}O$ ferromagnetic at room temperature (M_S becomes 5.6 emu/g of Mn when taking into account the Mn amount); finally in Ref. 7, a higher M_S value of 0.18 μ_B/Mn, has been reported for a 2 at. % Mn-ZnO sample. After these comparisons, it is possible to conclude that the ferromagnetic samples studied in this article lay in the typical magnetization range reported for the Mn-ZnO system.

X-ray absorption near-edge spectroscopy (XANES) experiments have been pointed out essentially in this field because they generate invaluable information on the dopant charge state.[5] XAS experiments were carried out in order to study the correlation between electronic and magnetic properties. For comparison purposes, Fig. 5(a) shows Mn *K*-edge XANES spectra of some reference compounds, a Mn metal foil, and several Mn oxides taken from the literature.[12] As shown in the inset of Fig. 5(a), these compounds provide a linear relationship between energy threshold and Mn valence state. However, the finding of the numerical value for the edge jump is troubled by the splitting of the $1s-4p$ transition[13] (labeled as *A* in the figure) that appears differently for each sample and affects the position of the first maximum of the first derivative. For that reason, the energy threshold has been estimated as the energy corresponding to one third of the jump. Figure 5(b) shows three films representative of ferromagnetic and paramagnetic behaviors. At first glance, it is clear that in the studied multilayers, first, Mn oxidation state differs from the metallic one; and second and more important, an edge energy shift is observed depending on the Mn layer thickness. It has obtained a shift of about 3.5 eV toward high energy from the thickest to the thinnest Mn-layer sample, which implies that, on average, Mn present in the samples has changed more than one valence state. By analyzing spectra with more detail, it can be observed that all Mn *K*-edge measurements corresponding to the studied samples show a less abrupt jump in comparison with references from pure valence states. These results suggest that Mn in the films is not in a pure valence state.[14] In this way, the obtained Mn oxidation state is the average of the actual distribution present in the sample, but even that average is very important to understanding the magnetic behavior.

A comparison between samples normalized XANES spectra with standard manganese oxide references allows an estimation of the average oxidation state. It should be noted that the entire depth of the film contributes to the measured XAS signal since the information depth is about 1 μm. This has been calculated for fluorescence collection under experimental conditions, defined in Ref. 15 (incoming beam incidence angle and outgoing fluorescence emission to detector angle are 45°). It means that, independently of their distance to the surface, all Mn atoms in the multilayers are contributing to the absorption signal and the obtained results (given in Table I) should be understood as corresponding to average Mn.

The obtained Mn oxidation states range between Mn^{2+} and Mn^{4+}. These results evidence that samples exhibiting ferromagnetic ordering have an average oxidation state near 2+ while the paramagnetic samples, obtained for the thinnest Mn layers, have a higher valence state. Similar results have been reported by Cong *et al.*[16] for ferromagnetic Mn-doped ZnO nanoparticles synthesized using the rheological phase reaction precursor method. By x-ray photoemission spectroscopy, they have found contributions of Mn^{2+}, Mn^{3+}, and Mn^{4+} in samples prepared with different Mn concentrations, being the most ferromagnetic sample the one having the largest Mn^{2+} concentration.

This variation of the Mn average oxidation state obtained by XANES is consistent with the Mn and ZnO growing conditions when preparing the studied multilayers. The growth of ZnO has been made by using a O_2/Ar mixture gas that remains a short time in the chamber after the layer growth. Under these conditions, the ZnO layers present a surface with absorbed oxygen, which become an oxidizing environment for the first steps of the following layer. When growing a thin Mn layer, the first deposited Mn may be easily oxidized and become near to the fully oxidized form (Mn^{4+}). Therefore, if Mn layer is sufficiently thin, highly oxidized Mn can be expected, but for higher thickness of manganese, it will tend to be in a reduced form. Conversely, a different situation is expected when ZnO starts to grow on

the Mn layer. ZnO diffusion into Mn layer can take place, but only Mn atoms very close to the upper interface may be oxidized, due to the competition between Mn and Zn to capture oxygen. In this case, it is expected to find Mn in a low oxidation state.

These different oxidation processes at the bottom and at the top of Mn layers are compatible with the obtained results. For thin enough Mn thickness (less than 15 Å) Mn^{4+} oxidation state results to be the predominant one [we have measured +3.3 for (30 Å ZnO/1 Å $Mn)_{75}$ sample]. However, when depositing a rather thick Mn layer (15–60 Å), an average Mn oxidation corresponding to its lowest oxidized form (Mn^{2+}) is expected. This fact, though, is compatible with Mn layer having a very small Mn^{4+} fraction deposited at the first growth stage.

Therefore, since interfaces at the bottom of the Mn layer are expected to be quite similar independent of the Mn layer thickness, the difference between films with higher ferromagnetic or paramagnetic component can be directly associated with these different Mn/ZnO interfaces at the top of Mn. As there is not any simple manganese oxide showing ferromagnetism above room temperature, it suggests that ferromagnetism is due to an interface effect under low Mn oxidation state condition. Moreover, results point toward ferromagnetism due to the formation of a ferromagnetic phase at the interface rather than a diluted magnetic semiconductor, even in the case of Mn thicknesses smaller than film roughness (about 7 Å). In principle, Mn diffusion into ZnO would be more likely in the case of very thin Mn layers, where layer thickness and interface roughness become comparable, favoring the cation diffusion process[8]; however, mostly paramagnetic behavior is observed in this case. This fact suggests that in the samples studied here, ferromagnetism is not caused by Mn diffusion into ZnO.

In addition, multilayers XANES spectra can be also compared with simulations of XANES based on multiple scattering in a structural model where Mn places in the Zn site of the low pressure wurtzite phase (tetrahedral coordination) as well as in the high pressure rocksalt phase (octahedral).[17] (30 Å ZnO/60 Å $Mn)_5$ sample XANES data seems to have some similarities with the obtained for an octahedral coordination. This fact suggests that a sample is mainly formed by a phase with octahedric Mn, but we cannot go further on the identification of that phase. (30 Å ZnO/7 Å $Mn)_{43}$ and (30 Å ZnO/1 Å $Mn)_{75}$ sample spectra are different, but they permit to assert that samples with very thin Mn layers (where all the small amount of Mn could be diffused in ZnO and contribute noticeably to the XANES features) no evidences of significant Mn substitution in ZnO phase are found by comparison with the simulations.

Nevertheless, (especially in samples with minority of ZnO) it can be expected that Zn diffuses into the thick enough manganese layers giving rise to a Zn-Mn-O ferromagnetic phase that develops at the ZnO/Mn interface. These results are not against the possibility of high temperature ferromagnetism in actual Mn:ZnO DMS. Nonetheless, they support the existence of complex oxides formed by Zn diffusion into manganese oxide[6,7] that has been reported by several authors as the source of high temperature ferromagnetism in Mn-Zn-O system.

IV. CONCLUSIONS

A series of Mn/ZnO multilayers prepared by sputtering shows paramagnetism or ferromagnetism depending on the manganese layer thickness. X-ray absorption spectroscopy (XANES) has been used to determine the Mn electronic properties, showing that the average oxidation state ranges from +2.1 to +3.3. This oxidation state can be correlated with the ferromagnetic or paramagnetic behavior of samples. It has been concluded that paramagnetic behavior is obtained when manganese is in a higher oxidation state while room temperature ferromagnetism is associated with Mn oxidation state close to +2. Ferromagnetism seems to be due to Mn/ZnO interface effect under low Mn oxidation state condition. Results seem to indicate the existence of a mixed Zn-Mn-O ferromagnetic phase at the interface rather than the formation of a diluted magnetic semiconductor.

ACKNOWLEDGMENTS

We thank the DGI-MEC for financial support under Contracts No. MAT2003-01880 and No. MAT2006-01004. J.G.L. acknowledges the "Ramon y Cajal" program of the Spanish MEC for financial support. We would like to thank Dr. N. D. Telling for the Xrealm software. Finally, we are grateful to the ESRF for making all facilities available.

[1] T. Dietl, H. Ohno, F. Matsukura, J. Cibert, and D. Ferrand, Science **287**, 1019 (2000).
[2] S. S. Kim, J. H. Moon, B. Lee, O. S. Song, and J. H. Je, J. Appl. Phys. **95**, 454 (2004).
[3] P. Sharma, A. Gupta, K. V. Rao, F. J. Owens, R. Sharma, R. Ahuja, J. M. O. Guillen, B. Johansson, and G. A. Gehring, Nat. Mater. **2**, 673 (2003).
[4] Z. Gu, M. Lu, J. Wang, D. Wu, S. Zhang, X. Meng, Y. Zhu, S. Shu, Y. Chen, and X. Pan, Appl. Phys. Lett. **88**, 082111 (2006).
[5] S. A. Chambers, Surf. Sci. Rep. **61**, 345 (2006).
[6] M. A. García, M. L. Ruiz-González, A. Quesada, J. L. Costa-Krämer, J. F. Fernández, S. J. Khatib, A. Wennberg, A. C. Caballero, M. S. Martín-González, M. Villegas, F. Briones, J. M. González-Calbet, and A. Hernando, Phys. Rev. Lett. **94**, 217206 (2005).
[7] D. C. Kundaliya, S. B. Ogale, S. E. Lofland, S. Dhar, C. J. Metting, S. R. Shinde, Z. Ma, B. Varughese, K. V. Ramanujachary, L. Salamanca-Riba, and T. Venkatesan, Nat. Mater. **3**, 709 (2004).
[8] S. S. Yan, C. Ren, X. Wang, Y. Xin, Z. X. Zhou, L. M. Mei, M. J. Ren, Y. X. Chen, Y. H. Liu, and H. Garmestani, Appl. Phys. Lett. **84**, 2376 (2004).
[9] A. B. Pakhomov, B. K. Roberts, and K. M. Krishnan, Appl. Phys. Lett. **83**, 4357 (2003).
[10] J. C. A. Huang, H. S. Hsu, Y. M. Hu, C. H. Lee, Y. H. Huang, and M. Z. Lin, Appl. Phys. Lett. **85**, 3815 (2004).
[11] E. Céspedes, C. Prieto, Y. Huttel, N. D. Telling, and G. van der Laan (to be published).
[12] D. A. McKeown and J. E. Post, Am. Mineral. **86**, 701 (2001).
[13] M. Croft, D. Sills, M. Greenblatt, C. Lee, S.-W. Cheong, K. V. Ramanujachary, and D. Tran, Phys. Rev. B **55**, 8726 (1997).
[14] J. Sánchez-Benítez, C. Prieto, A. de Andrés, J. A. Alonso, M. J. Martínez-Lope, and M. T. Casais, Phys. Rev. B **70**, 024419 (2004).
[15] R. Castañer and C. Prieto, J. Phys. III **7**, 337 (1997).
[16] C. J. Cong, L. Liao, J. C. Li, L. X. Fan, and K. L. Zhang, Nanotechnology **16**, 981 (2005).
[17] J. Pellicer-Porres, A. Segura, J. F. Sánchez-Royo, J. A. Sans, J. P. Itié, A. M. Flank, P. Lagarde, and A. Polian, Appl. Phys. Lett. **89**, 231904 (2006).